Binding Mode of [Ruthenium(II) (1,10-Phenanthroline)$_2$L]$^{2+}$ with Poly(dT*dA-dT) Triplex. Ligand Size Effect on Third-Strand Stabilization†

Sang-Doh Choi,‡ Myoung-Sun Kim,‡ Seog K. Kim,‡ Per Lincoln,§ Eimer Tuite,§ and Bengt Nordén*,§

Department of Chemistry, College of Sciences, Yeungnam University, Kyoungsan City, Kyoung-buk, 712-749, Republic of Korea, and Department of Physical Chemistry, Chalmers University of Technology, S-412 96 Gothenburg, Sweden

Received July 9, 1996; Revised Manuscript Received October 8, 1996⊗

ABSTRACT: The binding of homochiral [Ru(II)(1,10-phenanthroline)$_2$L]$^{2+}$ complexes {where L = 1,10-phenanthroline (phen), dipyrido[3,2-*a*:2′,3′-*c*]phenazine (DPPZ) or benzodipyrido[3,2-*a*:2′,3′-*c*]phenazine (BDPPZ)} to poly(dT*dA-dT) triplex has been investigated by linear and circular dichroism and thermal denaturation. Analysis of the linear dichroism spectra indicates that the extended DPPZ and BDPPZ ligands lie approximately parallel to the base-pair and base-triplet planes consistent with intercalation which is also supported by strong hypochromism in the interligand absorption bands with either duplex or triplex. The spectral properties of any of the metal complex enantiomers were similar for binding to either duplex or triplex DNA, indicating that the third strand, which occupies the major groove of the template duplex, has little effect on the binding geometries and hence supports the hypothesis that the metal complexes all bind from the minor groove with the DPPZ and BDPPZ ligands intercalated but without intercalation in the case of [Ru(phen)$_3$]$^{2+}$. Third-strand stabilization depended on the nature of the third substituted phenanthroline chelate ligand but was not directly related to its size, with stabilizing power increasing in the order phen < BDPPZ < DPPZ. This observation further supports intercalation of the extended ligands from the minor groove of the triplex since the extended BDPPZ ligand that would protrude into the major groove of the template would have greater steric interference than DPPZ with the third DNA strand.

Triple-helical DNA has been intensively studied due to the high selectivity of third-strand binding which presents a variety of potential applications in molecular biology, diagnostics, and therapeutics (Thuong & Hélene, 1993). Studies of drug interactions with triplex DNA are of importance for two reasons. The primary motivation is that in order to apply the triplex concept under physiological conditions, binding of the Hoogsteen base-paired strand must be stabilized and this can be achieved through intercalating drugs such ethidium dyes (Scaria & Shafer, 1991; Wilson et al., 1993; Tuite & Nordén, 1995a), acridines (Wilson et al., 1994; Kim et al., 1996) methylene blue (Tuite & Nordén, 1995b), coralyne (Lee et al., 1993), anthraquinones (Fox et al., 1995), naphthoquinolines (Wilson et al., 1993; Cassidy et al., 1994; Chandler & Fox, 1995; Chandler et al., 1995), or benzopyridoindole and -quinoxaline derivatives (Pilch et al., 1993a,b; Duval-Valentin et al., 1995; Escudé et al., 1995; Marchand et al., 1996). These compounds are reported to intercalate between the nucleobases of the triplex, thereby stablizing third-strand binding, and extended cresent-shaped compounds with some rotational flexibility are suggested to be the most effective stabilizers (Wilson et al., 1994). By contrast, most drugs that bind in the duplex minor groove probably also bind in the same site in the triplex but tend not to stablize the third strand (Umemoto et al., 1990; Wilson et al., 1993; Chalikian et al., 1994; Kim et al., 1996) except for berenil which is reported to stablize the third strand in the absence of NaCl (Durand et al., 1994; Pilch et al., 1995). However, the exact mechanisms by which drug binding stabilizes or destabilizes triplex have not yet been fully elucidated. A second motivation for studying drug−triplex interactions arises from interest in the structural motif of triplex DNA itself. In poly(dT*dA-dT) triplex (where * denotes the Hoogsteen base pairing and the dash denotes the Watson−Crick base pairing), the Hoogsteen paired poly(dT) third strand lies in the major groove of the template duplex, running parallel to the poly(dA) strand. Hence, third-strand binding changes the binding mode (Tuite & Nordén, 1995b) or may inhibit the binding (Kim & Nordén, 1993) of major groove interacting drugs.

The interactions of transition metal complexes containing planar aromatic ligands with DNA have been widely studies during the past decade (Nordén et al., 1996). In particular, octahedral ruthenium complexes[1] such as [Ru(phen)$_3$]$^{2+}$ which possess two isomers, *viz.* Δ- and Λ-enantiomers (Figure 1), have been investigated as probes of nucleic acid structure (Härd et al., 1987; Mei & Barton, 1988; Friedman et al., 1991; Naing et al., 1993), as artificial photonucleases (Kelly et al., 1985; Fleisher et al., 1986; Kelly et al., 1987, 1989; Tossi & Kelly, 1989; Chow & Barton, 1992; Feeney et al., 1994; Sentagne et al., 1994), as fluorescent hybridization probes (Bannwarth et al., 1988; Bannwarth, 1989; Freidman et al., 1990; Jenkins & Barton, 1992; Xu & Bard, 1995), and in electron transfer systems (Barton et al., 1986;

† This work is supported in part by the Basic Research Institute Program, Ministry of Education, Korea (Grant No. N96096 defrayed to S.K.K.). E.T. thanks EU HCM and Carl Trygger Foundation.

* Corresponding author. Tel: +46 31 772 3040. Fax: +46 31 772 3858. E-mail:norden@phc.chalmers.se.

‡ Yeungnam University.

§ Chalmers University of Technology.

⊗ Abstract published in *Advance ACS Abstracts,* December 1, 1996.

[1] Abbreviations: BDPPZ, benzodipyrido[3,2-*a*:2′,3′-*c*]phenazine; CD, circular dichroism; DPPZ, dipyrido[3,2-*a*:2′,3′-*c*]phenazine; LD, linear dichroism; phen, 1,10-phenanthroline; T_m, thermal denaturation temperature.

S0006-2960(96)01675-3 CCC: $14.00

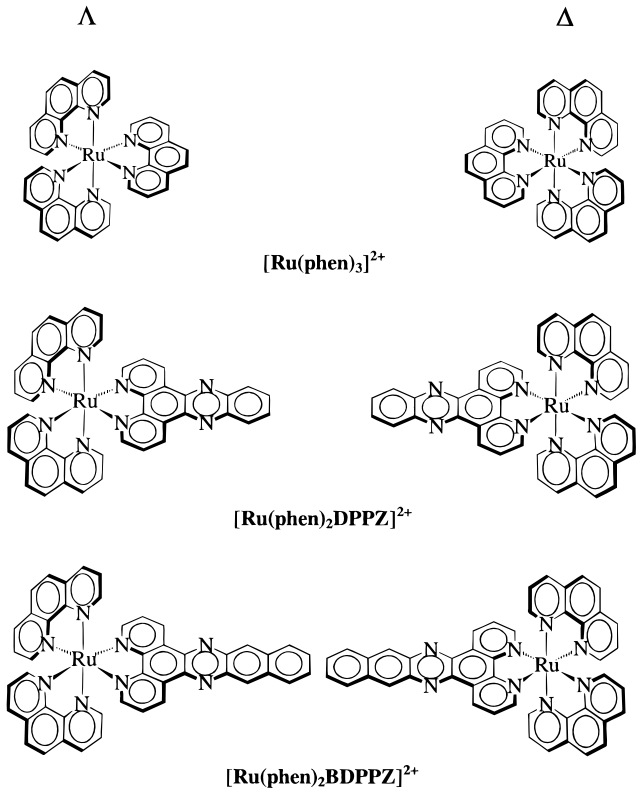

FIGURE 1: Molecular structures of the [Ru(II)(1,10-phenanthroline)$_2$L]$^{2+}$ complexes.

Purugganan et al., 1988; Kirsch-De Mesmaeker et al., 1990; Orellana et al., 1991; Lecomte et al., 1992; Murphy et al., 1993, 1994; Stemp et al., 1995; Arkin et al., 1996).

Despite much work, the mode of binding of the simple complex [Ru(phen)$_3$]$^{2+}$ to DNA remains an intensely controversial issue (Barton, 1986; Hiort et al., 1990; Rehmann & Barton, 1990; Haworth et al., 1991; Eriksson et al., 1992, 1994; Satyanarayana et al., 1992, 1993). Surface binding in the minor groove and intercalation of one 1,10-penanthroline ligand from the major groove was initially suggested (Barton, 1986; Rehmann & Barton, 1990), but classical intercalation of any ligand has been ruled out by viscosity measurements since neither enantiomer of [Ru(phen)$_3$]$^{2+}$ elongates short, rod-like DNA (Satyanarayana et al., 1992, 1993). Although partial intercalation of both enantiomers from the major groove was suggested by molecular modeling and energy minimization work (Haworth et al., 1991), a recent NMR and circular dichroism study shows that the interaction between the metal complex and DNA takes place primarily in the minor groove of the oligonucleotide without separation of the stacked bases (Eriksson et al., 1992, 1994).

However, when one of the ligands of the [Ru(phen)$_3$]$^{2+}$ complex is replaced by DPPZ or BDPPZ, the extended ligand undoubtedly intercalates between the DNA base pairs (Freidman et al., 1990; Jenkins et al., 1992; Hiort et al., 1993; Dupureur & Barton, 1994; Haq et al., 1995; Lincoln et al., 1996). Although intercalation from the major groove has been suggested for [Ru(phen)$_2$DPPZ]$^{2+}$ from NMR studies with a hexamer, our recent spectroscopic studies with T4 DNA, which is glycosylated in the major groove, have suggested that like [Ru(phen)$_3$]$^{2+}$ it binds from the minor groove (Tuite et al., in press).

The emission properties of racemic [Ru(bpy)$_2$DPPZ]$^{2+}$ and [Ru(phen)$_2$DPPZ]$^{2+}$ with poly(dT*dA-dT) have been reported previously (Jenkins et al., 1992). Increased luminescence enhancement of *rac*-[Ru(phen)$_2$DPPZ]$^{2+}$ upon binding to poly(dT*dA-dT) triplex compared to duplex has been assigned to increased protection of the DPPZ ligand from solvent afforded by base triplets which provide an extended surface area for stacking (Jenkins et al., 1992). Barton and co-workers (Jenkins et al., 1992) have assumed that these compounds bind to the new major groove of the triplex by analogy with model for duplex binding. However, since our recent studies (Tuite et al., in press) indicate instead minor groove binding of [Ru(phen)$_2$DPPZ]$^{2+}$, we consider it likely that this complex will bind to the triplex from the same groove.

In this study, we report spectroscopic evidence from linear and circular dichroism about the binding mode of the Δ- and Λ-enantiomers of three complexes[1] *viz.* [Ru(phen)$_3$]$^{2+}$, [Ru(phen)$_2$DPPZ]$^{2+}$, and [Ru(phen)$_2$BDPPZ]$^{2+}$ (Figure 1) with poly(dT*dA-dT) triplex and compare with their binding to [poly(dA-dT)]$_2$ duplex. These ruthenium complexes were chosen so that one phenanthroline ligand of the parent [Ru(phen)$_3$]$^{2+}$ complex is replaced with successively larger planar ligands (dipyridophenazine and benzodipyridophenazine) which exhibit strong intraligand absorption bands between 300 and 400 nm, thus enabling us to investigate ligand size effects on the binding mode using polarized spectroscopy. The effect of ligand size on the thermal stability of the third strand is also reported.

EXPERIMENTAL PROCEDURES

Materials

All chemicals and solvents were of analytical grade and used without further purification unless otherwise noted. All polynucleotides were purchased from Pharmacia and dissolved in 5 mM cacodylate buffer (pH 7.0) containing 100 mM NaCl and 1 mM EDTA and dialyzed several times against 5 mM cacodylate (pH 7.0) buffer. Poly(dT*dA-dT) triplex was prepared by incubating a 1:2 molar ratio mixture of poly(dA) and poly(dT) at 90 °C for 30 min followed by 24 h annealing at room temperature in 5 mM cacodylate buffer (pH 7.0) containing either 100 μM (for melting studies) or 150 μM $MgCl_2$ (for spectroscopic studies). Formation of the triplex was confirmed by its characteristic CD spectrum (Scaria & Shafer, 1991; Tuite & Nordén, 1995a) and melting profile. All measurements with poly[d(A-T)]$_2$ were performed in the same buffer but in the absence of $MgCl_2$. Polynucleotide concentrations were determined spectrophotometrically using the molar extintion coefficients: $\epsilon_{257nm} = 8600$ M^{-1} cm^{-1} for poly(dA), $\epsilon_{264nm} = 8520$ M^{-1} cm^{-1} for poly(dT), $\epsilon_{262nm} = 6600$ M^{-1} cm^{-1} for poly[d(A-T)]$_2$, and $\epsilon_{258nm} = 6600$ M^{-1} cm^{-1} for calf thymus DNA.

Syntheses of the homochiral ruthenium complexes have been described elsewhere (Hiort et al., 1990, 1993; Lincoln et al., 1996). Concentrations were determined using extinction coefficients of $\epsilon_{440nm} = 22\,000$ M^{-1} cm^{-1} for [Ru(phen)$_2$BDPPZ]$^{2+}$, $\epsilon_{439nm} = 20\,000$ M^{-1} cm^{-1} for [Ru(phen)$_2$DPPZ]$^{2+}$, and $\epsilon_{445nm} = 19\,000$ M^{-1} cm^{-1} for [Ru(phen)$_3$]$^{2+}$.

All spectroscopic measurements on the drug−polynucleotide samples were performed at mixing ratios, *R*, of [drug]/[base pair] or [drug]/[base triplet] of about 0.09. The concentrations of poly(dT*dA-dT) triplex and poly[d(A-T)]$_2$

duplex were 50 μM base triplet and base pair, respectively, for spectroscopic measurements. For melting profile measurements, the mixing ratio was 0.05 and the triplex concentration was 100 μM in adenine bases.

Absorption and Circular Dichroism (CD)

Absorption spectra were run on a Cary 2300 spectrophotometer. CD measurements were performed on either a Jasco J-720 or a Jasco J-500C spectropolarimeter (displaying the CD in millidegrees ellipticity). All triplex experiments were measured in the presence of 150 μM $MgCl_2$ to ensure a triple-helical conformation of the polynucleotide. The CD spectra of drug−polynucleotide mixtures provide information on two levels: (1) about the polynucleotide conformation itself which dominates the nucleobase absorption region due to excitonic interactions between electric transition moments of the nucleobases and (2) about the geometries of bound drug due to interactions between the transition moments of bound drug and the chirally arranged transition moments of nucleobases (Nordén et al., 1992; Nordén & Kurucsev, 1994).

Linear Dichroism (LD)

LD has proven to be a powerful technique for studies of binding geometries of drugs with polynucleotides (Nordén et al., 1992; Nordén & Kurucsev, 1994). LD is defined as the differential absorption of light polarized parallel and perpendicular to some laboratory reference axis, here the orientation axis of the sample. Reduced LD (LDr), which is defined as the (wavelength-dependent) ratio between the measured LD and the isotropic absorption spectrum, is related to the molar absortivity, $\epsilon_i(\lambda)$, of transition i at wavelength λ.

$$\mathrm{LDr} = \mathrm{LD}(\lambda)/A_{iso}(\lambda) = \Sigma_i f_i \epsilon_i(\lambda)\{\mathrm{LD}\}_i/\Sigma_i f_i \epsilon_i(\lambda) \quad (1)$$

where f_i is the fractional concentration of i. The angle, α, between the light-absorbing transition moments of polynucleotide-bound drug and, in the case of flow LD, the flow direction (polynucleotide helix axis) are related to the corresponding LDr according to

$$\{\mathrm{LDr}\}_i = 3S(3\langle\cos^2\alpha_i\rangle - 1)/2 \quad (2)$$

The brackets denote an ensemble average over the angular distribution. The orientation factor, S, reflects the degree of orientation of the polynucleotide in the flow. S is 1 for a perfectly oriented sample and 0 for an isotropic one. LD were measured on a Jasco-500A spectropolarimeter equipped and used as described elsewhere (Nordén & Seth, 1985). Polynucleotides were oriented in the flow with a gradient of 1800 s^{-1} using an outer rotating cylinder.

Melting Profiles

The dissociation (melting) of a polynucleotide strand from a double or triple helical polynucleotide manifests itself as absorption hyperchromism in the 260 nm wavelength region. Melting profiles were measured on an HP8452A diode array spectrophotometer equipped with an HP80890A Peltier temperature controller. The temperature was increased at a rate of 0.3 °C/3 min from 30 to 90 °C, with a reading taken 5 min after every temperature was attained.

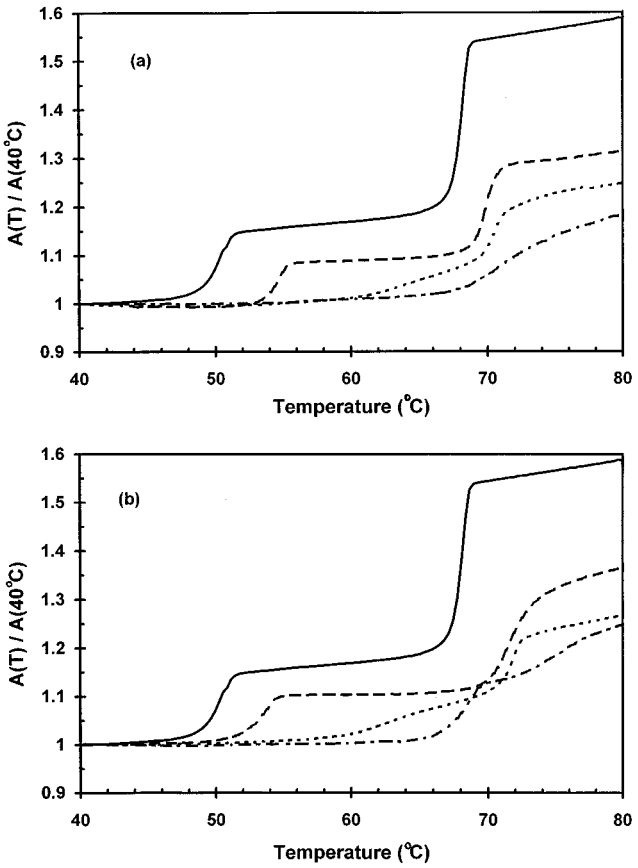

FIGURE 2: (a) Thermal melting profiles of triple helical poly(dT*dA-dT) in the absence (solid curve) and presence of the Δ-enantiomers of $[Ru(phen)_3]^{2+}$ (dashed curve), $[Ru(phen)_2DPPZ]^{2+}$ (alternating dot and dash curve), and $[Ru(phen)_2BDPPZ]^{2+}$ (dotted curve). The drug to polynucleotide triplet ratio is 0.05, and the concentration of the triplex is 100 μM in adenine base. (b) Thermal melting profiles of the Λ-enantiomers. The conditions and the concentrations are the same as for the Δ-enantiomers.

RESULTS

Thermal Denaturation Profiles

Dissociation (denaturation) of a duplex nucleic acid into two single strands or of a triplex nucleic acid into a duplex plus a single strand results in significant hyperchromism around 260 nm. Binding of a drug to a nucleic acid alters the denaturation temperatures depending on the strength of its interactions with the different nucleic acid conformations. Hence, thermal denaturation profiles provide a convenient means for detecting binding and also assessing relative binding strengths.

Under the conditions used in this study, the melting profile of triple-helical poly(dT*dA-dT) is biphasic (Figure 2), the first melting temperature (T_m) occurring at 51 °C and the second at 68 °C. The second T_m is confirmed to correspond to melting of the Watson−Crick base-paired duplex by comparison with a T_m of 65 °C for poly(dA)·poly(dT) duplex under the same conditions. Thus, the lower temperature T_m corresponds to the transition of poly(dT*dA-dT) triplex to poly(dA)·poly(dT) duplex + single-stranded poly(dT) *via* dissociation of the Hoogsteen base-paired poly(dT) strand from the major groove of the template duplex. Binding of any of the metal complexes studied results in both melting temperatures being raised to varying extents (Figure 2).

The T_m of the third strand increases to 54.5 and 53.5 °C and the second T_m increases to 70 and 72 °C upon adding,

respectively, the Δ- and Λ-enantiomers of [Ru(phen)$_3$]$^{2+}$ at a mixing ratio of 20 base triplets per complex. The effects of the intercalating complexes are more marked.

When one phenanthroline ligand is replaced by DPPZ, the first T_m increases significantly. With Δ-[Ru(phen)$_2$DPPZ]$^{2+}$, the effect is so strong that dissociation of the third strand does not occur before duplex dissociation, so that only a single broad transition is observed (73 °C). The DNA conformation at lower temperatures is confirmed to be triplex by its CD spectrum. With Λ-[Ru(phen)$_2$DPPZ]$^{2+}$, the stabilization of the third strand is somewhat less than with the Δ-enantiomer but is still strong enough to raise the first T_m to 69 °C. Denaturation of the Watson−Crick base-paired duplex occurs at 75 °C in presence of Λ-enantiomer. However, further expansion of the ligand size from DPPZ to BDPPZ results in a decrease of both the duplex and triplex stabilization effects, although triplex stabilization remains significantly greater than with [Ru(phen)$_3$]$^{2+}$. In the presence of [Ru(phen)$_2$BDPPZ]$^{2+}$, the first melting transition occurs over a broad temperature range with midpoint at 64 °C with Λ and 66 °C with Δ, and the second T_m occurs at 70.5 °C with Δ and 71.5 °C with Λ. Notably, while the Δ-enantiomers stabilize triplex more effectively, the Λ-enantiomers are more effective for stabilization of the template duplex.

Isotropic Absorption

In order to investigate further the source of ligand-dependent stabilization, spectroscopic measurements were made on these metal complex−nucleic acid systems. Figure 3 shows representative isotropic absorption spectra for the Λ-enantiomers of the metal complexes in the presence of poly(dT*dA-dT) triplex and poly[d(A-T)]$_2$ duplex. The absorption spectra of the relevant polynucleotides are subtracted from those of the mixtures. As previously reported for binding to duplex DNA (Hiort et al., 1990, 1993; Lincoln et al., 1996), the spectra of the Δ-enantiomers are essentially the same as those of the corresponding Λ-enantiomers and are not shown. All metal complexes exhibit hypochromism throughout the entire absorption region upon binding to either dupex or triplex. In the metal to ligand charge transfer region (MLCT band), some red-shifts are noticeable for the [Ru(phen)$_2$DPPZ]$^{2+}$ and [Ru(phen)$_2$-BDPPZ]$^{2+}$ complexes. Very strong hypochromism and red-shifts in the intraligand (DPPZ or BDPPZ) absorption bands for both enantiomers of [Ru(phen)$_2$DPPZ]$^{2+}$ (370 nm) (Figure 3b) and [Ru(phen)$_2$BDPPZ]$^{2+}$ (315 and 420 nm) (Figure 3c) indicate strong interactions between the nucleobases and, respectively, the DPPZ and BDPPZ ligands, consistent with an intercalation geometry for these extended ligands.

Linear Dichroism and Reduced Linear Dichroism

Linear dichroism (LD) spectra in the long-wavelength region for the Δ- and Λ-enantiomers of [Ru(phen)$_2$DPPZ]$^{2+}$ and [Ru(phen)$_2$BDPPZ]$^{2+}$ bound to flow-oriented poly-(dT*dA-dT) triplex and calf thymus DNA (CT-DNA) are depicted in Figure 4. To facilitate comparison, the LD spectra were normalized at wavelengths where the absorption is due to transitions polarized parallel to the long axis of the unique intercalating ligand and, therefore, the LD amplitude should be insensitive to a rotation about the 2-fold axis (340 nm for DPPZ and 330 nm for BDPPZ). Upon binding to

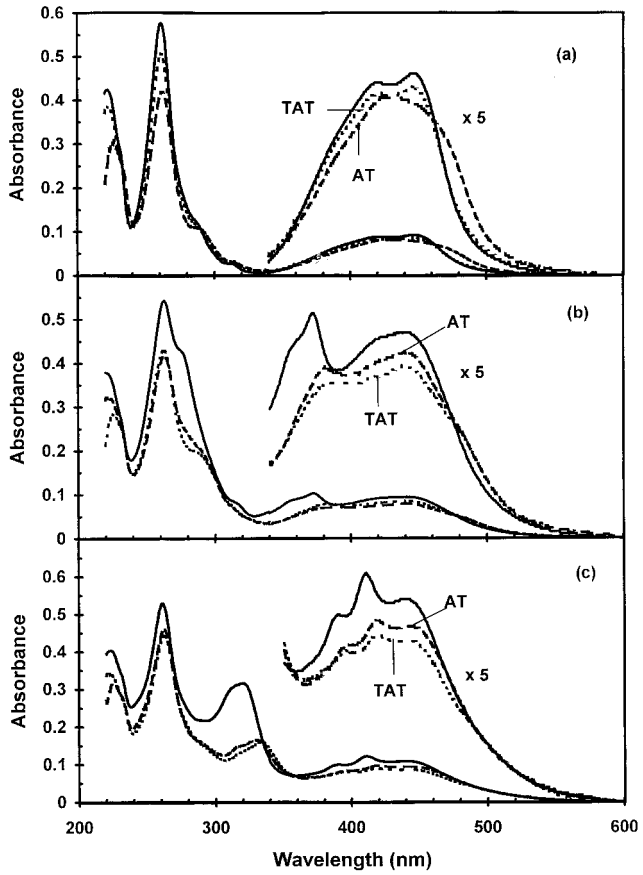

FIGURE 3: Absorption spectra of the Λ-enantiomers of (a) [Ru(phen)$_3$]$^{2+}$, (b) [Ru(phen)$_2$DPPZ]$^{2+}$, and (c) [Ru(phen)$_2$BDPPZ]$^{2+}$ bound to [poly(dA-dT)]$_2$ duplex (dashed curve, marked by AT) and to poly(dT*dA-dT) triplex (dotted curve, marked by TAT). The solid curve represents the profile for triplex in the absence of metal complex. The metal complex concentration is 4.5 μM, and the polynucleotide concentration is 50 μM in base pairs or base triplets. The absorption spectra of the relevant polynucleotides are subtracted.

DNA, the Λ-enantiomers of both [Ru(phen)$_2$DPPZ]$^{2+}$ and [Ru(phen)$_2$BDPPZ]$^{2+}$ exhibit negative LD between 300 and 380 nm, positive LD in the 380−460 nm region, and negative LD between 460 and 550 nm (Figure 4) (Hiort et al., 1993; Lincoln et al., 1996). The LD spectra for the the Λ-enantiomers bound to poly(dT*dA-dT) triplex are very similar to those with DNA, indicating that the binding geometries of the Λ-enantiomers complexed with DNA or poly(dT*dA-dT) are not significantly different.

The LD spectra of the Δ-enantiomers bound to DNA resemble those of the Λ-enantiomers, except in the intermediate wavelength region where the signals remain negative or close to zero. The spectra of the Δ-enantiomers bound to the poly(dT*dA-dT) triplex are somewhat different from those when bound to DNA, the LD between 400 and 500 nm being more negative with triplex as seen in Figure 4.

Figures 5 and 6 show the reduced linear dichroism (LDr) spectra of the Δ- and Λ-enantiomers, respectively, of (a) [Ru(phen)$_3$]$^{2+}$, (b) [Ru(phen)$_2$DPPZ]$^{2+}$, and (c) [Ru(phen)$_2$-BDPPZ]$^{2+}$ bound to poly(dT*dA-dT) triplex and to [poly-(dA-dT)]$_2$ duplex. The LDr spectra of all the complexes are heterogeneous, indicating the involvement of several electric transition moments of the metal complexes with different directionalities. The LDr magnitudes of both duplex and triplex in the polynucleotide absorption region decrease

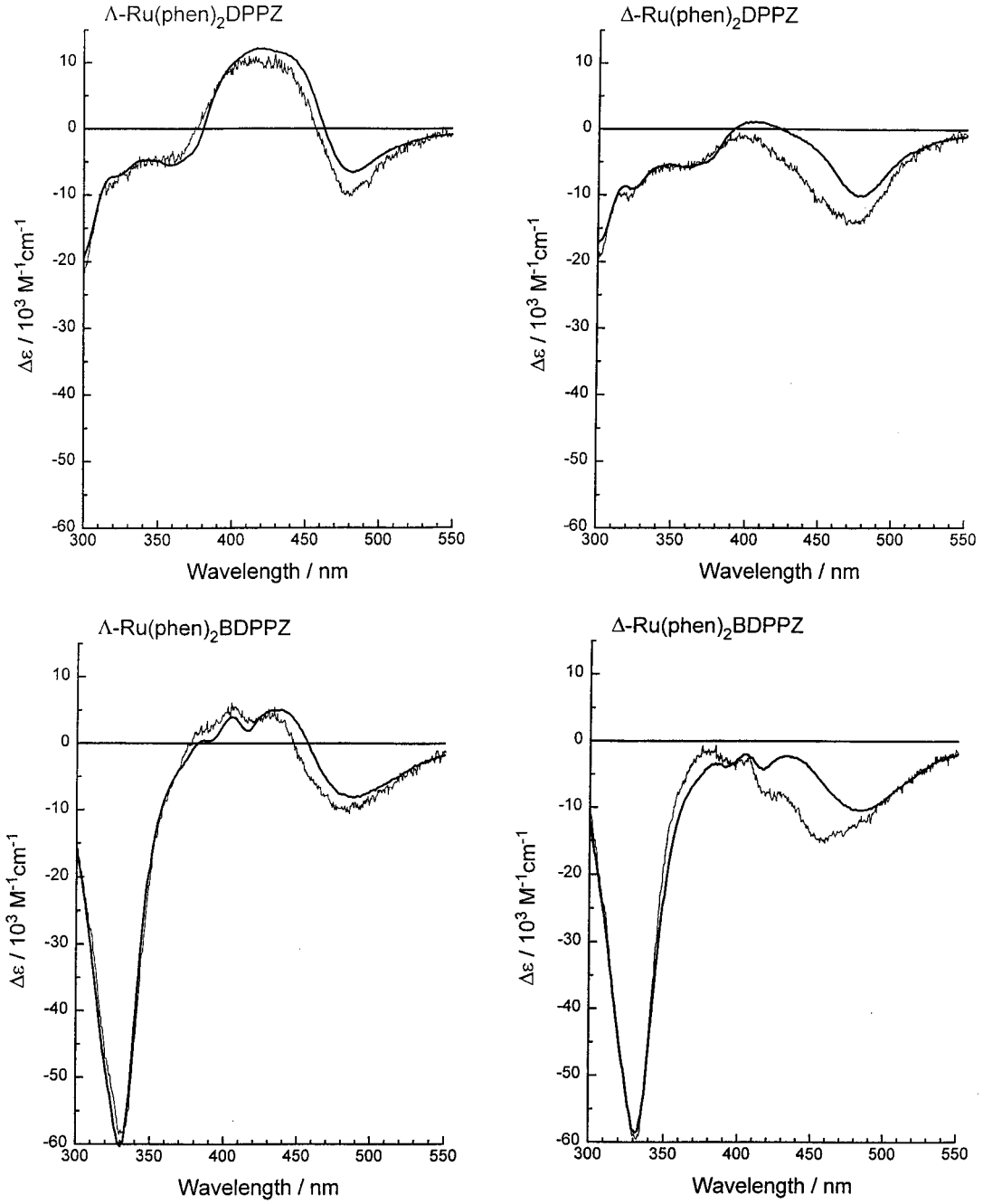

FIGURE 4: LD spectra determined for the enantiomers of $[Ru(phen)_2DPPZ]^{2+}$ (upper panel) and $[Ru(phen)_2BDPPZ]^{2+}$ (lower panel) bound to poly(dT*dA-dT) triplex (thin line) compared to spectra obtained with calf thymus DNA (thick curve). The spectra were normalized at 340 nm (DPPZ complexes) or at 330 nm (BDPPZ complexes), wavelengths where the LD signals are insensitive to a rotation around the 2-fold axis because the absorption is due to transitions polarized parallel to the long axes of the intercalating ligand.

significantly upon binding of the metal complexes. A positive contribution from the metal complexes which have strong positive LDr peaks around 260 nm (especially pronounced with triplex) may be partially responsible for the decrease in negative LDr magnitude. However, a lower LDr magnitude can also indicate a decrease of orientability when the complexes are bound which could be due to either increased flexibility or to more static bending of the polynucleotide induced by metal complex binding.

For $[Ru(phen)_2DPPZ]^{2+}$ and $[Ru(phen)_2BDPPZ]^{2+}$ bound to both poly(dT*dA-dT) triplex and $[poly(dA\text{-}dT)]_2$ duplex (Figures 5 and 6, b and c), in the 300−380 nm wavelength region, a strong negative LDr peak whose magnitude is as large as (or larger than) that in the polynucleotide absorption region is observed, indicating that the extended wing of the metal complex is perpendicular to the polynucleotide helix axis. For $[Ru(phen)_3]^{2+}$, the LDr signal in this region is too small to be analyzed (Figures 5a and 6a) due to the weak absorption of the metal complex in this region (Figure 3a). In the MLCT region, the shapes of the LDr spectra for each metal complex with triplex are similar to those with $[poly(dA\text{-}dT)]_2$ duplex, indicating similar binding geometries with both duplex and triplex. The LDr spectra of Δ-$[Ru(phen)_3]^{2+}$ bound to duplex or triplex polynucleotide consist of a positive band at short wavelength (∼380 nm) and a negative band at long wavelength (∼470 nm) (Figure 5a). The two bands are of approximately equal magnitude. For the Λ-enantiomer, a much smaller negative band at long wavelengths and a broad positive band (which is constant over a wide wavelength range) at short wavelengths are observed (Figure

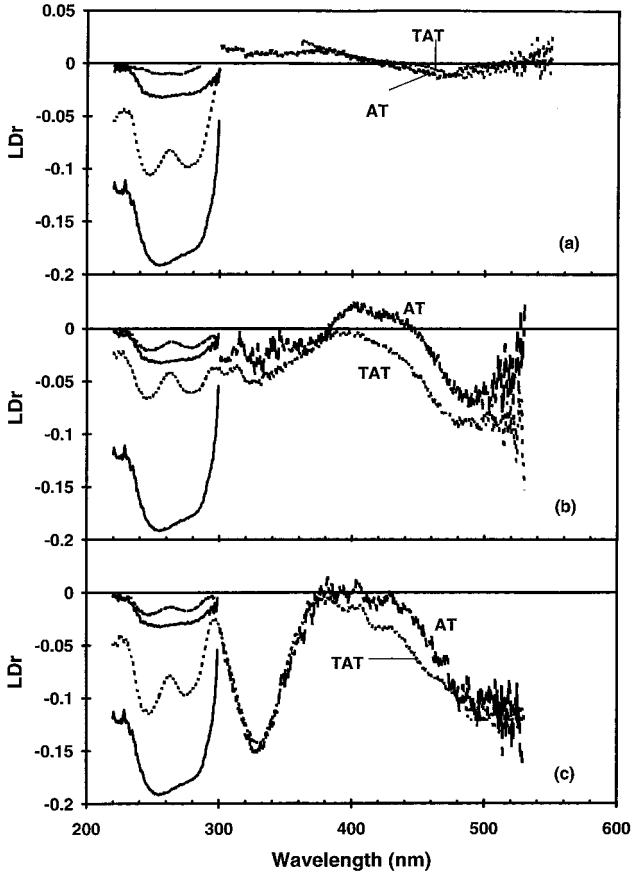

FIGURE 5: LDr spectra of the Δ-enantiomers of (a) [Ru(phen)$_3$]$^{2+}$, (b) [Ru(phen)$_2$DPPZ]$^{2+}$, and (c) [Ru(phen)$_2$BDPPZ]$^{2+}$ complexed with [poly(dA-dT)]$_2$ duplex and poly(dT*dA-dT) triplex. The concentrations and the curve assignments are the same as in Figure 3 except for the signal in the polynucleotide absorption region which is (from bottom) the LDr of free triplex, triplex in presence of the metal complex, free duplex, and duplex in presence of the metal complex. The signal above 300 nm for the metal complex bound to duplex is normalized relative to the signal of the triplex complex at 280 nm to facilitate comparison.

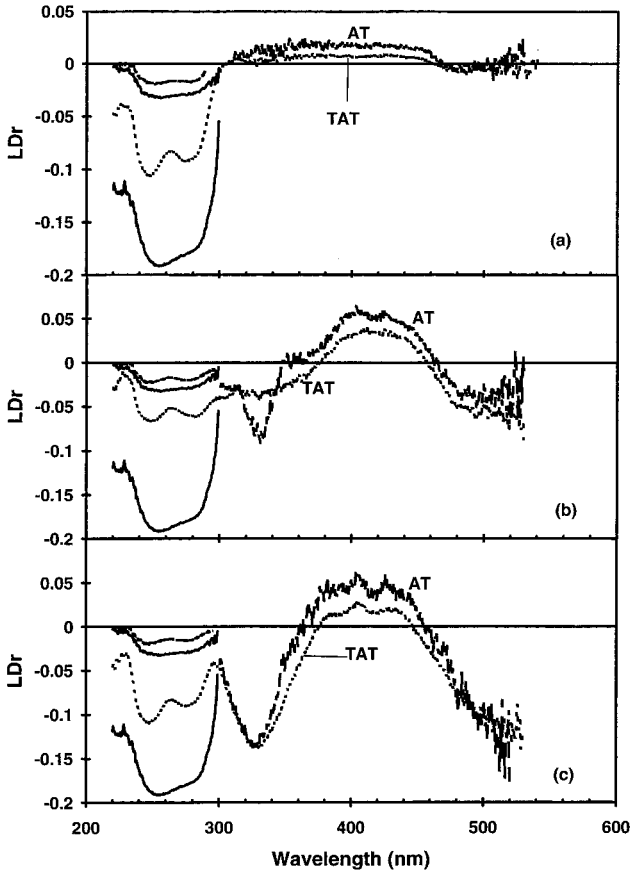

FIGURE 6: LDr spectrum of the Λ-enantiomers complexed with [poly(dA-dT)]$_2$ duplex and poly(dT*dA-dT) triplex. The conditions are the same as in Figure 5.

5a). These features are similar to previously reported spectra with CT-DNA (Hiort et al., 1990).

Δ-[Ru(phen)$_2$DPPZ]$^{2+}$ and Δ-[Ru(phen)$_2$BDPPZ]$^{2+}$ bound to both duplex and triplex exhibit similar LDr properties above 380 nm consisting of an almost zero LDr around 400 nm and strong negative values at longer wavelengths (Lincoln et al., 1996). The LDr spectra of the Λ-enantiomers are quite similar to those of the Δ-enantiomers except that the nearly zero LDr around 400−450 nm becomes positive for the Λ-enantiomers.

Circular Dichroism

Circular dichroism (CD) spectra of the metal complexes in the presence of the duplex and triplex polynucleotides are depicted in Figures 7 and 8. The CD spectra of the corresponding polynucleotides are substracted from the spectra of the mixtures. In this report, we limit ourselves to discussing the CD changes in the MLCT bands because changes of the CD spectra in the short-wavelength region (<320 nm) may originate from either the polynucleotide or the metal complex. In the MLCT band of the CD spectrum of Δ-[Ru(phen)$_3$]$^{2+}$, binding to [poly(dA-dT)]$_2$ duplex produces a positive change in the long-wavelength region (∼450 nm) and a small negative change in the short-wavelength region (∼420 nm) (Figure 7a). For Λ-[Ru(phen)$_3$]$^{2+}$, positive changes in both the long- and short-wavelength regions are observed (Figure 8a). These data are in agreement with previously published spectra (Hiort et al., 1990). When [Ru(phen)$_3$]$^{2+}$ enantiomers are bound to poly(dT*dA-dT) triplex, similar changes are observed (to a somewhat smaller extent) except in the long-wavelength region for the Λ-enantiomer where the CD intensity decreases slightly upon binding (Figures 7a and 8a). The CD changes in the MLCT bands of [Ru(phen)$_2$DPPZ]$^{2+}$ (Figure 7b for Δ- and Figure 8b for Λ-enantiomer) and [Ru(phen)$_2$BDPPZ]$^{2+}$ (Figure 7c for Δ- and Figure 8c for Λ-enantiomer) in presence of the polynucleotide are quite similar to those of [Ru(phen)$_3$]$^{2+}$ bound to the respective polynucleotide.

DISCUSSION

Electronic Transition Moments of the [Ru(phen)$_2$L]$^{2+}$ Chromophore

The strong, broad absorption band centered around 440 nm of the ruthenium bipyridyl type complexes is due to several d→π* metal to ligand charge transfer (MLCT) transitions and the absorption in the UV region (around 260 nm) to $\pi\rightarrow\pi$* intra-ligand transitions (Krausz & Ferguson, 1989). An intra-ligand $\pi\rightarrow\pi$* transition polarized along the C_2 symmetry long axis of the complex [*A* direction (Lincoln et al., 1996)] is responsible for the strong absorption bands at 350 and 310 nm of [Ru(phen)$_2$DPPZ]$^{2+}$ and [Ru(phen)$_2$BDPPZ]$^{2+}$, respectively, in their DNA complexes (Lincoln et al., 1996).

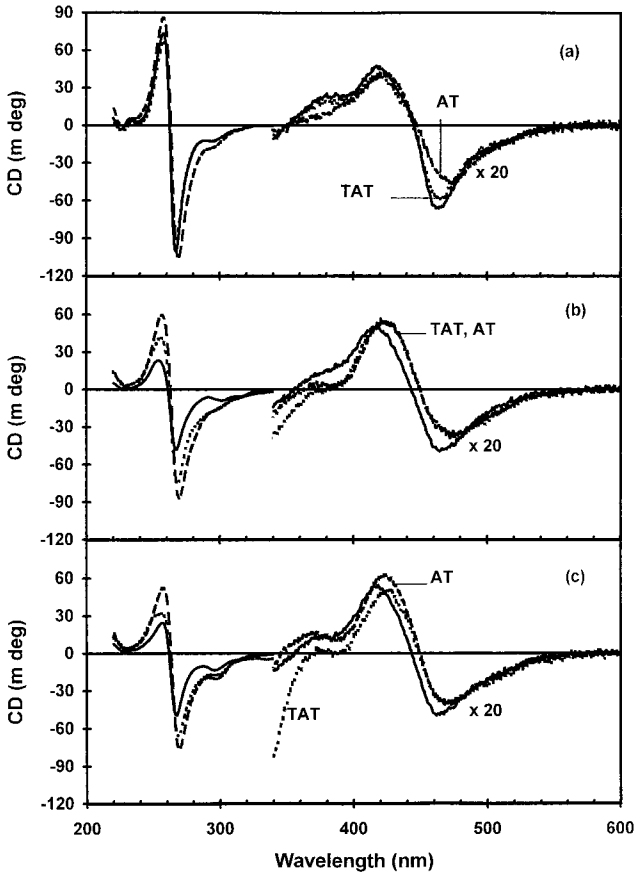

FIGURE 7: CD spectra of the Δ-enantiomers of (a) $[Ru(phen)_3]^{2+}$, (b) $[Ru(phen)_2DPPZ]^{2+}$, and (c) $[Ru(phen)_2BDPPZ]^{2+}$ free in solution (solid curves), bound to $[poly(dA\text{-}dT)]_2$ duplex (dashed curve, marked by AT), and bound to poly(dT*dA-dT) triplex (dotted curve, marked by TAT). Concentrations are the same as in Figure 3. Path length 1 cm. The CD spectra of the relevant polynucleotides are subtracted from those of the mixtures.

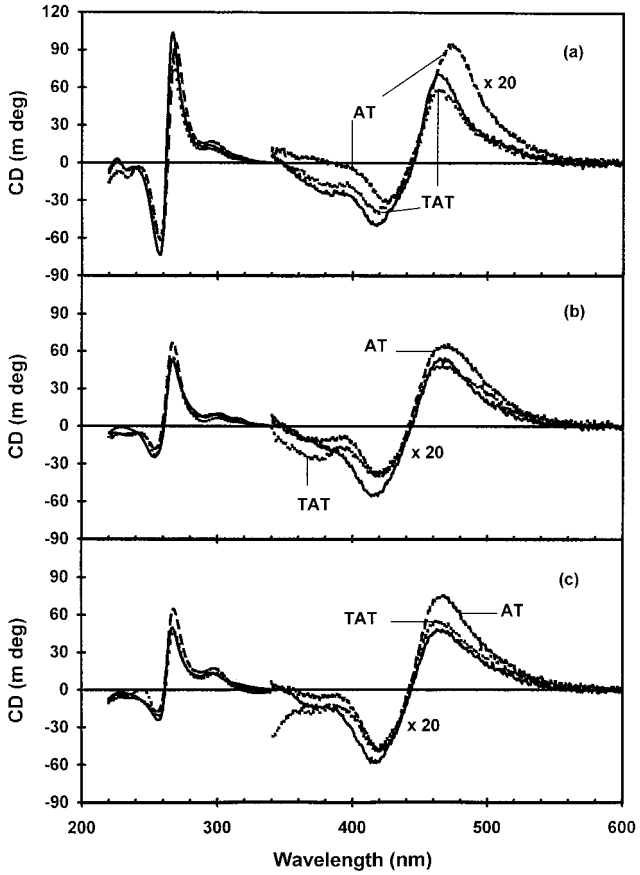

FIGURE 8: CD spectra of the Λ-enantiomers. The conditions and curve assignments are the same as in Figure 7.

Absorption and CD

In the presence of polynucleotide, the magnitude and shape of the visible absorption bands of the ruthenium complexes are noticeably altered compared to those of polynucleotide-free metal complexes. For each of the complexes, the spectral changes for the two enantiomers differ only slightly from each other, indicating that the environment of the polynucleotide-bound enantiomers and their interactions with nucleobases are not very different. The dependence of changes in the visible absorption band (Figure 3a of both $[Ru(phen)_3]^{2+}$ enantiomers on the nature of the polynucleotide suggests some differences in the interactions of this complex with poly(dT*dA-dT) triplex and with $[poly(dA\text{-}dT)]_2$ duplex. On the other hand, the shapes of the absorption spectra of either $[Ru(phen)_2DPPZ]^{2+}$ (Figure 3b) or $[Ru(phen)_2BDPPZ]^{2+}$ (Figure 3c) are similar in the presence of triplex or duplex, showing slightly higher hypochromicities in the triplex case. Hence, it appears that as ligand size increases, it is the interaction between intercalated ligand and the nucleobases, rather than the nature of polynucleotide (whether duplex or triplex), thet is the dominant determinant of the metal complex binding mode.

The origin of the induced CD signal when a compound interacts with a nucleic acid is complicated and very sensitive to the environment of the bound ligand (Lyng et al., 1991, 1992). With enantiomeric metal complexes there is the further complication of an intrinsic CD in the absence of polymer which may be perturbed on binding to DNA. Changes in the MLCT bands of the metal complex CD spectra upon binding to polynucleotide may result from either structural or electronic perturbations. Changes in the CD spectra in the MLCT region (460 nm) are "unsymmetric" (Figures 7 and 8). For example, for $[Ru(phen)_3]^{2+}$ there is a large positive change with duplex for both Δ- and Λ-enantiomers, while with triplex there is a small negative change for Δ and a small negative change for Λ. A similar trend is observed for $[Ru(phen)_2DPPZ]^{2+}$ and $[Ru(phen)_2BDPPZ]^{2+}$. The magnitudes of the CD signals at 310 nm for $[Ru(phen)_2BDPPZ]^{2+}$ and at 385 nm for $[Ru(phen)_2DPPZ]^{2+}$ are too small to be analyzed. Although binding to duplex and triplex cause slightly different variations in the CD spectra of the complexes, suggesting that subtle differences exist in the binding interactions, it is extremely difficult to interpret such small CD variations in terms of differences in binding geometry due to the complex origin of CD.

The changes in the band at 260 nm may be more revealing since here there are notable differences in the behaviors of the Δ- and Λ-enantiomers. $[Ru(phen)_2DPPZ]^{2+}$ and $[Ru(phen)_2BDPPZ]^{2+}$ both increase the exciton CD for the Δ-enantiomer bound to duplex and triplex but the difference is smaller with $[Ru(phen)_3]^{2+}$ as well as with all the Λ-enantiomers. This may be an indication that the DNA structure is structurally perturbed by binding of the Δ-enantiomers of the intercalating metal complexes.

Binding Geometry from LD and LDr

We have recently analyzed in some detail the LD spectra of $[Ru(phen)_2DPPZ]^{2+}$ and $[Ru(phen)_2BDPPZ]^{2+}$ when bound

to calf thymus DNA (Lincoln et al., 1996). A strong MLCT band, polarized at 55° to the plane of the (B)DPPZ ligand, was found to be a sensitive indicator of any short axis inclination of this ligand from an all-perpendicular orientation relative to the helix axis. The substantial difference between the LD spectra of the enantiomers at ∼400 nm is due to the fact that a small clockwise roll of the intercalated ligand short axis moves this transition closer to the orientation axis for the Λ-complex (more positive LD) but away from the orientation axis for the Δ-enantiomer.

The comparable magnitude and the negative sign in the LDr spectra of the large DPPZ (and BDPPZ) ligand in $[poly(dA\text{-}dT)]_2$ duplex and poly(dT*dA-dT) triplex indicate undoubtedly that the strong intra-ligand transition polarized along the symmetry long axis of the complex lies almost parallel to the polynucleotide base plane. Together with the strong hypochromicity that is specific for the $\pi\rightarrow\pi^*$ transition of the large ligand, this is indicative of intercalation of the ligand between the polynucleotide base pairs. The shapes of the LD spectra of the metal complexes with triplex are quite similar to those with calf thymus DNA (especially for the Λ-enantiomers, Figure 4), indicating that the binding geometry of the metal complexes in the poly(dT*dA-dT) triplex is not very different from that in DNA.

Roll angles, defined as the clockwise rotation about the 2-fold axis of the complex and measured as the angle between the polynucleotide helix axis and the normal to the (B)DPPZ ligand plane, were calculated by the method described previously (Lincoln et al., 1996). The roll angles of Λ-$[Ru(phen)_2DPPZ]^{2+}$ and Λ-$[Ru(phen)_2BDPPZ]^{2+}$ complexed with triplex are, respectively, +13° and +7°, which are about the same as those observed with duplex DNA. On the other hand, roll angles of Δ-$[Ru(phen)_2DPPZ]^{2+}$ and Δ-$[Ru(phen)_2BDPPZ]^{2+}$ with DNA are +7° and +5°, respectively, which increase to +13° and +10° upon binding to the triplex, indicating that the Δ-enantiomers are slightly more tilted in the triplex compared to duplex DNA. The shapes of the LDr spectra of the DPPZ- and BDPPZ-containing metal complexes (Figure 5 and 6, b and c) bound to triplex are similar to those when bound to $[poly(dA\text{-}dT)]_2$ duplex, again indicating that the binding geometries with duplex and triplex are not very different.

The negative LDr magnitude of both $[poly(dA\text{-}dT)]_2$ duplex and poly(dT*dA-dT) triplex decreases by up to as much as half upon binding of the metal complexes. This may be partly due to a positive LDr contribution in the DNA band from the bound metal complexes. Another factor that can reduce the LDr magnitude is reduced orientability of the polynucleotide which could be due either to increased flexibility, due to local denaturation for example, or to static bending of the polynucleotide upon binding of the compound. However, in all cases where linear dichroism has been used to study binding to the poly(dT*dA-dT) triplex, the compounds have been reported to reduce the LD magnitude which is related to the orientation of the polynucleotide. This is observed not only for intercalators such as ethidium bromide (Tuite & Nordén, 1995a), methylene blue (Tuite & Nordén, 1995b), and acridines (Kim et al., 1996) but also for groove-binders such as DAPI and Hoechst (Kim et al., 1996). Hence, with triplex, it is not possible to draw any conclusions about the binding geometry from such an observation.

Binding of the non-intercalating $[Ru(phen)_3]^{2+}$ complex also results in a decrease of the LD magnitude for both duplex or triplex, similar to binding of the intercalating metal complexes. With duplex DNA, the reduction in orientation by Δ-$[Ru(phen)_3]^{2+}$ (Hiort et al., 1990) was suggested to arise from kinking of the DNA at the metal complex binding site since the viscosity of DNA was also observed to decrease (Satyanarayana et al., 1992, 1993) Λ-$[Ru(phen)_3]^{2+}$, by contrast, was reported to have little effect on either orientation (Hiort et al., 1990) or viscosity (Satyanarayana et al., 1992, 1993). Intercalation is expected to lengthen DNA, and indeed binding of either $[Ru(phen)_2DPPZ]^{2+}$ enantiomer results in increased DNA viscosity (Haq et al., 1995) although the effects on orientation measured by LD are small and depend on enantiomer (Lincoln et al., 1996). The reduction in duplex orientation observed with the $[Ru(phen)_2DPPZ]^{2+}$ and $[Ru(phen)_2BDPPZ]^{2+}$ enantiomers could potentially arise from perturation of the DNA structure, perhaps kinking or bending at the site of binding. If it is the bulkiness of $[Ru(phen)_3]^{2+}$ in the minor groove that causes DNA to bend, then this bend may be less marked with $[Ru(phen)_2DPPZ]^{2+}$ and $[Ru(phen)_2BDPPZ]^{2+}$ because for these complexes intercalation causes DNA to lengthen and the groove to expand, consistent with the minor effects observed with the latter complexes. We note that actinomycin D also intercalates with bulky groups residing in the minor groove causing DNA to bend somewhat (Kamitori & Takusagawa, 1994). Further detailed studies using hydrodynamic techniques are necessary to investigate any DNA perturbation effects in greater depth.

Denaturation Profiles

Binding of intercalators such as ethidium (Scaria & Shafer, 1991; Wilson et al., 1994; Tuite & Nordén, 1995a), acridines (Wilson et al., 1994; Kim et al., 1996), methylene blue (Tuite & Nordén, 1995b), coralyne (Lee et al., 1993; Wilson et al., 1994), ellipticine (Wilson et al., 1994), naphthoquinoline derivatives (Wilson et al., 1993), and benzopyridoindole derivatives (Pilch et al., 1993a,b) to the poly(dT*dA-dT) triplex results in increased thermal stability of the triplex structure. Although the mechanism of triplex DNA stabilization by intercalators is not clear, a few factors can be hypothesized: (1) good stacking interactions between the base triplets and the intercalator; (2) tethering of the third strand *via* hydrogen bond formation with an intercalator which is anchored between the bases of the template duplex; (3) cationic nature of most intercalators combined with (4) the separation of negative backbone charges inherent to intercalation (due to elongation and unwinding of the nucleic acid) which may help overcome unfavorable electrostatics for third-strand association. Even though it cannot intercalate, $[Ru(phen)_3]^{2+}$ does somewhat stabilize the third-strand binding, indicating that the third factor is involved in the triplex stabilization mechanism. Hence, changes in solvent structure and the counter-ion distribution about the phosphate group caused by dication binding probably account for at least part of the triplex stabilization by the metal complexes. When $[Ru(phen)_2DPPZ]^{2+}$ is complexed with triplex, the DPPZ wing is large enough to be fully intercalated. Pronounced increases in the T_m of the third strand upon replacing the third phenanthroline ligand with DPPZ indicate the importance of the first, and possibily also the second, hypothesis. However, the role of hydrogen bond formation

between the intercalator and the third strand is likely to be of minor importance since we have observed that for acridine derivatives, changing the nature and position of substituents, which could possibly form hydrogen bonds with the third strand, does not significantly affect the melting profiles of the poly(dT*dA-dT) triplex (to be published).

When the DPPZ wing is extended further to BDPPZ, the triplex stabilization effect decreases. If the metal complexes intercalate from the minor groove, as we suggest (see next section), there may be steric clashes between the extended BDPPZ ligand protruding into the major groove of the template duplex and the third strand that binds in that groove. The geometry of the bound $[Ru(phen)_2BDPPZ]^{2+}$ may not allow as good stacking of BDPPZ with the base triplets as can be achieved by DPPZ. Notably, each of the metal complexes, particularly {$[Ru(phen)_2DPPZ]^{2+}$ ($[Ru(phen)_2$-$BDPPZ]^{2+}$ does not enhance the duplex stability more than $[Ru(phen)_3]^{2+}$} also increases the duplex denaturation temperature significantly. From the data presented here, it is clear that increasing the surface area of an intercalating ligand is not sufficient to improve its triplex-stabilizing capability but can instead have the opposite effect. Rather, the ligand should be designed to have maximal overlap with the base triplets.

Binding Mode of the Metal Complexes with Triplex

It is clear from the spectroscopic data that the planes of the extended ligands of $[Ru(phen)_2DPPZ]^{2+}$ and $[Ru$-$(phen)_2BDPPZ]^{2+}$ are nearly parallel to the nucleobase plane (perpendicular to the polynucleotide helix axis) for both enantiomers with poly(dT*dA-dT) triplex as well as with CT-DNA and $[poly(dA\text{-}dT)]_2$. A great deal of evidence indicates that the extended ligands are intercalated with duplex DNA: viscometry of DNA with $[Ru(phen)_2DPPZ]^{2+}$ showing elongation of DNA upon complex binding (Haq et al., 1995), although this is not the case with $[Ru(phen)_3]^{2+}$ (Satyanarayana et al., 1992, 1993), and unwinding of supercoiled DNA (Friedman et al., 1991) as well as strong hypochromism in the absorption spectrum, particularly in the intraligand band (Hiort et al., 1993; Lincoln et al., 1996). Since the spectral characteristics of the metal complexes bound to poly(dT*dA-dT) triplex are so similar to those bound to DNA and $[poly(dA\text{-}dT)]_2$ duplex, we conclude the binding modes are not significantly different between the various nucleic acids.

The final question we address is from which direction are the metal complexes intercalated? NMR studies (Eriksson et al., 1994) place $[Ru(phen)_3]^{2+}$ in the minor groove of duplex DNA without intercalation and the similarity of the spectroscopic properties suggests the same binding to triplex. Although NMR (Dupureur & Barton, 1994) and simple model building (Jenkins et al., 1992) suggest that DPPZ intercalated duplex DNA from the major groove, our recent photophysical studies (Tuite et al., in press) suggest instead that it also binds from the minor groove. Furthermore, a major groove binding model can not explain the dependence of the third-strand stabilization effect on the ligand size. Therefore, we propose that the DPPZ ligand of the metal complexes is intercalated with the two phenanthroline ligands located in the minor groove of the polynucleotide, thereby stablizing the third strand by expansion of the stacking interaction. The smaller stabilizing effect of $[Ru(phen)_2$-$BDPPZ]^{2+}$ may thus be attributed to the steric interference of the protruding ligand with the third strand in the major groove. Furthermore, it has been observed that drugs which bind in the major groove of poly(dT*dA-dT) such as methylene blue (Tuite & Nordén, 1995b) and methyl green (Kim & Nordén, 1993) exhibit large spectral changes when the major groove of the template duplex is filled by the third strand. No such changes were observed with any of the complexes under study here. On the other hand, the intercalators and minor groove binding drugs have similar spectral properties whether bound to duplex or to triplex (Tuite & Nordén, 1995a; Kim et al., 1996) which is consistent with observations for the metal complexes if they interact with DNA from the minor groove.

CONCLUSION

The DPPZ and BDPPZ wings of the ruthenium complexes intercalate between the nucleobases when bound to poly-(dT*dA-dT) triplex, thereby stabilizing the third strand. The binding geometries of the metal complexes in triplex DNA, with the plane of the intercalating ring system approximately parallel to the plane of the base triplet and rotated slightly clockwise around the complex C_2 axis, are not very different from those in duplex DNA with similar, minor variations between the enantiomers. From the wing size effect on the melting profile the other two phenanthroline ligands of the metal complexes are proposed to be located in the minor groove of the triplex poly(dT*dA-dT). This conclusion is supported by the similar binding geometries and also similar diastereomeric perturbations of the CD spectra observed in the duplex and triplex cases.

REFERENCES

Arkin, M. R., Stemp, E. D. A., Turro, C., Turro, N. J., & Barton, J. K. (1996) *J. Am. Chem. Soc. 118*, 2267−2274.

Bannwarth, W. (1989) *Anal. Biochem. 181*, 216−219.

Bannwarth, W., Schmidt, D., Stallard, R. L., Hornung, C., Knorr, R., & Müller, F. (1988) *Helv. Chim. Acta 71*, 2085−2099.

Barton, J. K. (1986) *Science 233*, 727−734.

Barton, J. K., Kumar, C. V., & Turro, N. J. (1986) *J. Am. Chem. Soc. 108*, 6391−6393.

Cassidy, S. A., Strekowski, L., Wilson, W. D., & Fox, K. R. (1994) *Biochemistry 33*, 15338−15347.

Chalikian, T. V., Plum, G. E., Sarvazyan, A. P., & Breslauer, K. J. (1994) *Biochemistry 33*, 8629−8640.

Chandler, S. P., & Fox, K. R. (1995) *FEBS Lett. 360*, 21−25.

Chandler, S. P., Strekowski, L., Wilson, W. D., & Fox, K. R. (1995) *Biochemistry 34*, 7234−7242.

Chow, C. S., & Barton, J. K. (1992) *Methods Enzymol. 212*, 217−242.

Dupureur, C. M., & Barton, J. K. (1994) *J. Am. Chem. Soc. 116*, 10286−10287.

Durand, M., Thuong, N. T., & Maurizot, J. C. (1994) *J. Biomol. Struct. Dyn. 11*, 1191−1202.

Duval-Valentin, G., de Bizemont, T., Takasugi, M., Mergny, J. L., Bisagni, E., & Hélene, C. (1995) *J. Mol. Biol. 247*, 847−858.

Eriksson, M., Leijon, M., Hiort, C., Nordén, B., & Gräslund, A. (1992) *J. Am. Chem. Soc. 114*, 4933−4934.

Eriksson, M., Leijon, M., Hiort, C., Nordén, B., & Gräslund, A. (1994) *Biochemistry 33*, 5031−5040.

Escudé, C., Nguyen, C. H., Mergny, J.-L., Sun, J.-S., Bisagni, E., Garestier, T., & Hélene, C. (1995) *J. Am. Chem. Soc. 117*, 10212−10219.

Feeney, M., M., Kelly, J. M., Tossi, A. B., Kirsch-De Mesmaeker, A., & Lecomte, J.-P. (1994) *J. Photochem. Photobiol. B: Biol. 23*, 69−78.

Fleisher, M. B., Waterman, K. C., Turro, N. J., & Barton, J. K. (1986) *Inorg. Chem. 25*, 3549−3551.

Fox, K. R., Polucci, P., Jenkins, T. C., & Neidle, S. (1995) *Proc. Natl. Acad. Sci. U.S.A. 92*, 7887−7891.
Freidman, A. E., Chambron, J.-C., Sauvage, J.-P., Turro, N. J., & Barton, J. K. (1990) *J. Am. Chem. Soc. 112*, 4960−4962.
Friedman, A. E., Kumar, C. V., Turro, N. J., & Barton, J. K. (1991) *Nucleic Acids Res. 19*, 2595−2602.
Haq, I., Lincoln, P., Suh, D., Nordén, B., Chowdhry, B. Z., & Chaires, J. B. (1995) *J. Am. Chem. Soc. 117*, 4788−4796.
Härd, T., Hiort, C., & Nordén, B. (1987) *J. Biomol. Struct. Dyn. 5*, 89−96.
Haworth, I. S., Elcock, A. H., Freeman, J., Rodger, A., & Richards, W. G. (1991) *J. Biomol. Struct. Dyn. 9*, 23−44.
Hiort, C., Nordén, B., & Rodger, A. (1990) *J. Am. Chem. Soc. 112*, 1971−1982.
Hiort, C., Lincoln, P., & Nordén, B. (1993) *J. Am. Chem. Soc. 115*, 3448−3454.
Jenkins, Y., & Barton, J. K. (1992) *J. Am. Chem. Soc. 114*, 8736−8738.
Jenkins, Y., Freidman, A. E., Turro, N. J., & Barton, J. K. (1992) *Biochemistry 31*, 10809−10816.
Kamitori, S., & Takusagawa, F. (1994) *J. Am. Chem. Soc. 116*, 4154−4165.
Kelly, J. M., McConnell, D. J., OhUigin, C., Tossi, A. B., Kirsch-De Mesmaeker, A., Masschelein, A., & Nasielski, J. (1987) *J. Chem. Soc., Chem. Commun.*, 1821−1823.
Kelly, J. M., Tossi, A. B., McConnell, D. J., & OhUigin, C. (1985) *Nucleic Acids Res. 13*, 6017−6034.
Kelly, J. M., Tossi, A. B., McConnell, D. J., OhUigin, C., Helene, C., & Le Doan, T. (1989) in *Free Radicals, Metal Ions and Biopolymers* (Beaumont, P. C., Deeble, D. J., Parsons, B. J., & Rice-Evans, C., Eds.) pp 143−156, Richelieu Press, London.
Kim, H.-K., Kim, J.-M., Kim, S. K., Rodger, A., & Nordén, B. (1996) *Biochemistry 35*, 1187−1194.
Kim, S. K., & Nordén, B. (1993) *FEBS Lett. 315*, 61−64.
Kirsch-De Mesmaeker, A., Orellana, G., Barton, J., & Turro, N. J. (1990) *Photochem. Photobiol. 52*, 461−472.
Krausz, Z., & Ferguson, J. (1989) *Prog. Inorg. Chem. 37*, 293−390.
Lecomte, J.-P., Kirsch-De Mesmaeker, A., Kelly, J. M., Tossi, A., & Görner, H. (1992) *Photochem. Photobiol. 55*, 681−689.
Lee, J. S., Latimer, L. J. P., & Hampel, K. J. (1993) *Biochemistry 32*, 5591−5597.
Lincoln, P., Broo, A., & Nordén, B. (1996) *J. Am. Chem. Soc. 118*, 2644−2653.
Lyng, R., Rodger, A., & Nordén, B. (1991) *Biopolymers 31*, 1709−1720.
Lyng, R., Rodger, A., & Nordén, B. (1992) *Biopolymers 32*, 1201−1214.
Marchand, C., Bailly, C., Nguyen, C. H., Bisagni, E., Garestier, T., Hélene, C., & Waring, M. J. (1996) *Biochemistry 35*, 5022−5032.
Mei, H.-Y., & Barton, J. K. (1988) *Proc. Natl. Acad. Sci. U.S.A. 85*, 1339−1343.
Murphy, C. J., Arkin, M. R., Jenkins, Y., Ghatlia, N. D., Bossmann, S. H., Turro, N. J., & Barton, J. K. (1993) *Science 262*, 1025−1029.
Murphy, C. J., Arkin, M. R., Ghatlia, N. D., Bossmann, S., Turro, N. J., & Barton, J. K. (1994) *Proc. Natl. Acad. Sci. U.S.A. 91*, 5315−5319.
Naing, K., Takahashi, M., Taniguchi, M., & Yamagishi, A. (1993) *J. Chem. Soc., Chem. Commun.*, 402−403.
Nordén, B., & Seth, S. (1985) *Appl. Spectrosc. 39*, 647−655.
Nordén, B., & Kurucsev, T. (1994) *J. Mol. Recognit. 7*, 141−156.
Nordén, B., Kubista, M., & Kurucsev, T. (1992) *Q. Rev. Biophys. 25*, 51−170.
Nordén, B., Lincoln, P., Åkerman, B., & Tuite, E. (1996) in *Metal Ions in Biological Systems* (Sigel, A., & Sigel, H., Eds.) pp 177−252, Marcel Dekker, Inc., New York.
Orellana, G., Kirsch-De Mesmaeker, A., Barton, J. K., & Turro, N. J. (1991) *Photochem. Photobiol. 54*, 499−509.
Pilch, D. S., Martin, M.-T., Nguyen, C. H., Sun, J.-S., Bisagni, E., Garestier, T., & Hélene, C. (1993a) *J. Am. Chem. Soc. 115*, 9942−9951.
Pilch, D. S., Waring, M. J., Sun, J.-S., Rougée, M., Nguyen, C.-H., Garestier, T., & Hélene, C. (1993b) *J. Mol. Biol. 232*, 926−946.
Pilch, D. S., Kirolos, M. A., & Breslauer, K. J. (1995) *Biochemistry 34*, 16107−16124.
Purugganan, M. D., Kumar, C. V., Turro, N. J., & Barton, J. K. (1988) *Science 241*, 1645−1649.
Rehmann, J. P., & Barton, J. K. (1990) *Biochemistry 29*, 1701−1709.
Satyanarayana, S., Dabrowiak, J. C., & Chaires, J. B. (1992) *Biochemistry 31*, 9319−9324.
Satyanarayana, S., Dabrowiak, J. C., & Chaires, J. B. (1993) *Biochemistry 32*, 2573−2584.
Scaria, P. V., & Shafer, R. H. (1991) *J. Biol. Chem. 266*, 5417−5423.
Sentagne, C., Chambron, J.-C., Sauvage, J.-P., & Paillous, N. (1994) *J. Photochem. Photobiol. B: Biol. 26*, 165−174.
Stemp, E. D. A., Arkin, M. R., & Barton, J. K. (1995) *J. Am. Chem. Soc. 117*, 2375−2376.
Thuong, N. T., & Hélene, C. (1993) *Angew. Chem., Int. Ed. Engl. 32*, 666−690.
Tossi, A. B., & Kelly, J. M. (1989) *Photochem. Photobiol. 49*, 545−556.
Tuite, E., & Nordén, B. (1995a) *Bioorg. Med. Chem. 3*, 701−711.
Tuite, E., & Nordén, B. (1995b) *J. Chem. Soc., Chem. Commun.*, 53−54.
Tuite, E., Lincoln, P., & Nordén, B. *J. Am. Chem. Sci.* (in press).
Umemoto, K., Sarma, M. H., Gupta, G., Lao, J., & Sarma, R. H. (1990) *J. Am. Chem. Soc. 112*, 4539−4545.
Wilson, W. D., Mizan, S., Tanious, F. A., Yao, S., & Zon, G. (1994) *J. Mol. Recognition 7*, 89−98.
Wilson, W. D., Tanious, F. A., Mizan, S., Yao, S., Kiselyov, A. S., Zon, G., & Strekowski, L. (1993) *Biochemistry 32*, 10614−10621.
Xu, X.-H., & Bard, A. J. (1995) *J. Am. Chem. Soc. 117*, 2627−2631.

BI961675A